Hindawi
Wireless Communications and Mobile Computing
Volume 2022, Article ID 1755053, 11 pages
https://doi.org/10.1155/2022/1755053

*Research Article*

# Estimation of Harvested RF Energy Based on Survey of Ambient RF Power for Optimized Rectifier Design

**Kirote Arpanutud,[1] Sitt Tontisirin,[2] Nonchanutt Chudpooti,[3] and Suramate Chalermwisutkul[1]**

[1]*The Sirindhorn International Thai-German Graduate School of Engineering, King Mongkut's University of Technology North Bangkok, Bangkok, Thailand*
[2]*Silicon Craft Technology Public Company Limited, Bangkok, Thailand*
[3]*Faculty of Applied Science, King Mongkut's University of Technology North Bangkok, Bangkok, Thailand*

Correspondence should be addressed to Suramate Chalermwisutkul; suramate.c@tggs.kmutnb.ac.th

Received 5 August 2022; Revised 17 November 2022; Accepted 22 November 2022; Published 30 November 2022

Academic Editor: Muhammad Inam Abbasi



This paper presents estimation of harvested RF energy by means of measurement survey and rectifier circuit simulation. The survey was done in an indoor environment in Bangkok, Thailand using a low-cost in-house developed measurement system. From the survey, channel power distribution of a signal with 950 MHz center frequency and 20 MHz bandwidth was created. The maximum time averaged channel power is -7.6 dBm whereas the mean value with maximum signal statistic is -11.1 dBm. A single stage rectifier is simulated with 5 different nominal values of RF input power which is used to optimize the rectifier for maximum RF-to-DC power conversion efficiency. The rectifier composes a Schottky diode, a matching network and a simple load consisting of a resistor and a storage capacitor. Parameters of the simplified LC matching network have been varied to match the rectifier's input impedance to 50 Ω for various nominal values of the RF input power. In addition, the load resistance was varied according to the nominal RF input power for an optimal power conversion efficiency of the rectifier. The rectifier delivers the highest harvested RF energy with a nominal RF input power of -9 dBm which is a value between the maximum and the mean values from the survey. The DC energy converted from ambient RF energy by the rectifier can be estimated. With this information, it can be assessed what type of applications based on available RF energy can be applied for the test area. This rectifier optimization strategy can be applied to any kind of RF signal since it is based on actual measurement results. Moreover, the proposed rectifier can be designed for reconfigurability regarding nominal RF input power at the location of interest by varying the matching network parameters and the load resistance. In practical applications, the reconfigurable rectifier can maintain a high level of power conversion efficiency over a wide range of RF input power. This can be done by optimizing the rectifier's input matching network and the load resistance for the highest possible power harvested from the environment where the rectifier is located.

## 1. Introduction

Radio frequency energy harvesting (RFEH) has been of great interest for researchers since its concept was introduced. However, applying the concept for real applications is very challenging due to extremely small amount of harvestable RF energy. The amount of ambient RF energy that can be harvested is relatively small compared to other ambient sources e.g., solar energy, mechanical vibration, and temperature difference [1, 2]. Thus, the major purpose of RFEH is the energy supply for sensor nodes with low power consumption where light, vibration, temperature difference, and other sources of energy are not available. The most prominent application of RFEH is radio frequency identification (RFID). The passive RFID tags are attached to objects which can wirelessly be identified by RFID readers. Without the need of a battery, a passive tag harvests the RF energy transmitted by the reader to activate the RFID chip with

the object's digital identification. By regulations, the transmitted power of the reader is limited whereas activation of the RFID chip on the tag requires a certain amount of energy. The work reported in [3] proposed the technique of using self-oscillating antennas serving as additional wireless energy sources for RFID tags. With additional wireless energy sources, the read range can be increased or additional functionalities e.g., temperature or moisture sensing can be added to the tags [4, 5]. In wireless sensor networks, battery time of the sensor nodes e.g., wearable sensors can be prolonged by reducing their power consumption or by including the RFEH capability in the devices [6–8]. In general, the power consumption of a wireless sensor node ranges from 1 to 12 mW depending on their applications [9, 10]. Test measurements of average ambient RF power reported in the surveys from [11, 12] show the range of ambient RF power from 6 uW to 0.35 mW. However, these values were not considered as design parameters of the rectifier, an electronic circuit which converts the ambient RF input signal to direct current (DC). As for instantaneous values, the ambient RF power varies depending on location and time of the measurement. In [11–14] the measurement time was set to the longest possible. After data acquisition, the values were averaged to represent the overall test result. The test methods in [14, 15] referred to standard mobile base station measurement without focusing on a survey for harvestable ambient RF power. It is also required that the locations of RF transmitters are known. Considering the receiving antenna for ambient RF power measurement, directional, omnidirectional, or isotropic radiation patterns can be used [16]. In case of a directional antenna, the maximum received power must be specified by rotating the antenna until the maximum value is found [12, 13]. If different types and configurations of antenna for the survey are used, the survey results at the same location are different. Theoretically, any type of antenna can be used for the survey measurement given that the antenna provides a sufficient gain so that available frequency bands for RFEH can be identified with a sufficient signal to noise ratio. An omnidirectional and circularly polarized antenna is normally chosen as an antenna for the survey measurement of the field strengths to assess potential harmful electromagnetic irradiation. In that case, electric and magnetic field strengths in any direction and polarization must be measured and evaluated. For RFEH, an omnidirectional and circularly polarized antenna can ensure that the RF energy can be harvested from signals coming from any direction and orientation of the fields. However, by adjusting the direction and orientation of the receiving antenna using a linearly polarized, directional antenna, higher amount of RF energy can be harvested compared to an omnidirectional and circularly polarized receiving antenna. The drawback in such a case is that tuning of the antenna direction and orientation must be performed every time when the RFEH device is placed at a new location. In addition, the situation of propagation also changes from time to time as new mobile base stations or Wi-Fi routers are installed in the area of interest. Another method to enhance the amount of harvested RF energy is using a wideband antenna combined with a wideband rectifier. However, designing a wideband rectifier is complicated since many rectifiers apply the narrowband harmonic rejection technique or resonance circuits to enhance the power conversion efficiency [17]. Besides, large amount of RF energy is usually not available over a large bandwidth but rather in a few specific frequency bands. Thus, the practical use of a wideband antenna for RFEH lies in the freedom to combine it with a rectifier operating at any frequency band that is covered by the bandwidth of the antenna [18]. More promising is the multiband antenna array where each array element is dedicated for RFEH from a single frequency channel with high amount of RF energy [19, 20]. A measurement survey to find the frequency channels with promising RF power is required for this concept. If the frequency channels of interest are not much different in terms of center frequency, a single wideband antenna combined with separate signal paths with dedicated impedance matching for each frequency channel can also be applied [21].

The RF power captured from free air by the antenna is delivered to the rectifier. RF to DC power conversion efficiency (PCE) of a rectifier has a crucial impact on the entire RFEH system performance. To optimize the PCE of a rectifier, typical RF input power during the harvesting time and in the harvesting area must be known. Similar to power added efficiency of a RF power amplifier, PCE of a rectifier increases with increasing RF input power until the maximum value is reached. By increasing the RF input power beyond this optimum point, PCE decreases rapidly as voltage swing over the diode, the rectifier's main power conversion device, reaches its breakdown [22]. Another key parameter of the diode for RFEH rectifier design is the threshold voltage. If the voltage swing over the diode reaches a higher value than the threshold voltage, the diode is turned on allowing electric current to flow through the device. The level of voltage swing across the diode depends mainly on the DC load and the RF input power. On the diode's IV curve, the voltage swing resulting from the RF input power and the DC load can be plotted as the so-called load line [23]. If the diode is not turned on since the RF input power is too low or the load impedance is too high, the RF to DC conversion does not take place and the PCE drops to zero. Significant efforts have been made on the device level to lower, cancel, or compensate the diode's threshold voltage so that the rectifier can convert very small amount of RF input power to DC [24]. Low threshold devices are mainly used for RFID chips for read range extension rather than for RFEH. If the rectifier is designed to provide the highest PCE at the maximum RF power of the ambient signal, as the signal power fluctuates over time and positions, the power backoff leads the reduced PCE of the rectifier. Therefore, prior to design of the rectifier, an extensive survey needs to be carried out to gain insights in available frequency bands, RF input power level and its distribution over time and positions. This information is crucial for estimation of harvestable RF energy and assessment of practical applications in the area of interest. Also, choice of the diode and its operating point with the maximum PCE requires information regarding RF input power distribution from the survey to obtain reasonably high amount of harvested RF energy.

In the literature, few surveys dedicated to RFEH have been presented [11, 12]. None of them presented the RF input power distribution from the survey as a design parameter for RFEH rectifiers. In this work, harvested RF energy converted to DC by the rectifier is estimated using survey results of ambient RF input power. A compact, low-cost measurement system was developed to capture and process the measurement data of the survey. To reduce the complexity of the measurement procedure, the antenna used in this work has an omnidirectional radiation pattern. The antenna gain was determined using the gain transfer method [25]. The measurement result of ambient RF channel power was normalized to exclude the receiving antenna gain from the measured data. Data structure has been designed to visualize and evaluate large amounts of measured data. The most promising frequency channel for RFEH with the highest channel power was selected. Time averaged channel power acquired from the survey was used to optimize the RF to DC power conversion efficiency (PCE) in the rectifier design process. A simulation study of the rectifier designed based on the survey results is presented to demonstrate the PCE optimization technique according to the measured average RF input power. We show that the survey is very important to assess whether RFEH is worth doing in the first place in the area of interest. If so, the survey result also reveals RF input power distribution as important information for the rectifier optimization. This technique can be applied to signals of any wireless communication standard since it is based on actual measurement results.

## 2. Power Conversion Efficiency of a Rectifier as a Function of RF Input Power

It is commonly known that available channel power at a position varies over time due to the nonconstant signal envelope of mobile communication signals. The power level is also different considering day and night-time as well as in different time of the year. For rectifier circuit design, it is important to know the input power at which the PCE should be optimized. The loss mechanism of the diode has been presented in [22] and depicted in Figure 1. The horizontal axis in Figure 1 represents the variation of RF input power fed to the rectifier by the receiving antenna. As the input power is gradually increased, the diode changes from the OFF state to the ON state so that a small amount of diode current starts to flow. As the input power increases, the diode current also increases. When the state transition is completed, the diode current and the PCE of the rectifier reach their maximum at an optimal level of the input power. If the input power exceeds this optimal value, the voltage swing across the diode is entering the breakdown region. The lower half of the voltage waveform is clipped and PCE drops sharply as the input power is further increased. It is noted that the plot in Figure 1 assumes a constant load resistant RL of the rectifier. The effect of the load resistance to PCE is presented in [26] as plots of PCE over RL and in [23] as a PCE contour over the input power and RL.

PCE of a rectifier can be maintained over a wide range of RF input power by combining several rectifiers optimized

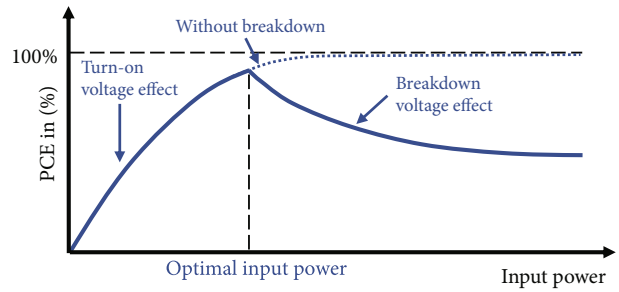


Figure 1: Loss mechanism of a diode in a rectifier circuit.

for maximum PCE at different input power levels. RF input power from the receiving antenna is fed either to the low-power or the high-power rectifier depending on the power level. The signal path can be controlled by a transistor operated as a switch [27] or by power dividers and power selective matching networks [28]. The low-power rectifier uses a diode with low turn-on voltage for a high PCE at low input power level. The breakdown voltage of such a device is also low; so that PCE is decreased as the input power is increased. To prevent further decrease of PCE, the high-power rectifier is activated as the input power exceeds the predefined threshold. Thus, high PCE can be maintained at high input power level since the diode used in high-power rectifier has a higher turn-on voltage and a higher breakdown voltage. The rectifier concept with adaptive path control is illustrated in Figure 2. This method is more useful for wireless power transfer (WPT) applications with dedicated RF power transmitter since the expected level of available RF power is known and beam of the transmission antenna can be directed to the receiver. The receiver of a commercially available WPT kit [29] shows 55% PCE in the low-power mode with -6 dBm optimal input power and 62% in the high-power mode with 3 dBm input power. In this case, the goal is to maintain high PCE in a wide range of distance between transmitter and receiver.

In case of RFEH, the input power is much lower since no dedicated RF power transmitter is available. Since the ambient RF power fluctuates over time, it is important to know distribution of the power level. The power distribution of a single transmitter depends on the number of tones and modulation scheme of the signal. In [30], PCE of a fabricated rectifier for RFEH was measured by feeding single tone, multitone, and digitally modulated signals directly into the rectifier's RF input. In [31], single tone, multitone with low peak to average power ratio, and random and chaotic signals were converted to DC using a commercial WPT receiver and a commercial antenna to evaluate PCE of all signals under test. However, the rectifiers in those works were prefabricated and not custom designed based on actual ambient signals with different power distributions.

High ambient RF power level is more promising for RFEH than low power level since it is more straightforward to optimize the rectifier's PCE. Low signal power level with low signal statistic can be neglected in the rectifier design process. In this case, the amount of harvested RF energy, even with a high PCE, is extremely small so that no practical application is possible. For the same reason, optimizing PCE at a low input

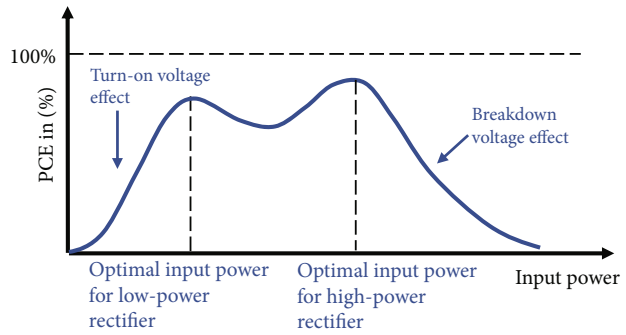


Figure 2: PCE over input power of a rectifier with adaptive path control.

power while using a limiter to prevent the diode from entering the breakdown region is also not an option since the peak RF power is wasted. A better strategy is to optimize the rectifier at a specific RF input power to harvest reasonable amount of energy by considering the RF power distribution from the survey measurement in the area of interest.

## 3. Survey of Ambient RF Power

Due to small amount of ambient RF energy, the most promising frequency channel should be selected for RFEH. The measurement area in this work is located on the 4th floor of the Sirindhorn International Thai-German Graduate School of Engineering (TGGS), King Mongkut's University of Technology North Bangkok in Bangkok, Thailand. At this state, no outdoor measurement has been considered since it requires an official permission to perform the measurement in public spaces. The indoor scenario is also more of interest for the industrial partner of our project.

The test area is illustrated in Figure 3 left which is derived from the floorplan obtained from the building management. This area was divided into 42 subareas in which the average ambient RF energy was measured. The measurement equipment was placed at the center of each subarea where the measurement was performed over the testing time. After the measurement of a subarea was completed, the measurement equipment was moved to the next subarea to perform the measurement again until the entire area is covered. All subareas are assigned with letter-number coordinates from a1 to k4 to evaluate the ambient RF energy of each position. The average value over a certain time of the ambient RF energy can be plotted for each position. The distribution of RF power in the entire test area is represented as a color pattern referred to as a *heat map* where the color scale represents level of the RF power of each coordinates' position.

The RF power of each position was measured for two minutes using a monopole antenna and 3G Combo compact spectrum analyzer (SPA) from RF Explorer™ [32]. A minicomputer Raspberry PI model B+ with a touch screen was used to control the SPA as well as to store and postprocess the measurement data. The block diagram and a photograph of the measurement system is shown in Figure 4 consisting of the low-cost SPA and a raspberry PI model B+ with a touch screen.

The measured raw data of the received power is referred to as $P_{\text{INraw}}$ which can be expressed as a product of the power density $s_t$ from the transmission side and the effective capture area $A_{\text{er}}$ of the receiving antenna.

$$P_{\text{INraw}} = s_t \cdot A_{\text{er}}. \tag{1}$$

The effective capture area depends on the receiving antenna gain which is a monopole in our case. The antenna gain varies over the frequency $f$ and is referred to as $G_{\text{mono}}(f)$. For simplification, the gain is assumed to be constant at the center frequency of the channel. The effective capture area can be expressed as

$$A_{\text{er}} = \frac{G_{\text{mono}}(f)\lambda^2}{4\pi}, \tag{2}$$

where $f$ and $\lambda$ are the measurement frequency and its corresponding wavelength, respectively. Thus, to calculate the incident power density $s_t$ from the measured RF input power $P_{\text{INraw}}$, the receiving antenna gain is required according to the following formular

$$s_t = \frac{4\pi P_{\text{INraw}}}{G_{\text{mono}}(f)\lambda^2}. \tag{3}$$

*3.1. Monopole Antenna Used for Power Density Measurement.* The antenna used for the survey must be characterized to determine its gain at the measurement frequency. The antenna was measured in an anechoic chamber as shown in Figure 5.

By applying the gain-transfer method referred to the standard horn antenna HF907 from Rohde and Schwarz, the gain of the test antenna can be determined for four frequency channels; 869-894 MHz, 940-960 MHz, 1,805-1,880 MHz, and 2,110-2,170 MHz which are the major frequency channels allocated for mobile communication in Thailand. For all frequency channels, the radiation patterns are near to omni directional. The gain of each band was averaged over the frequency and azimuth angle to simplify evaluation of the measured data. The average gains of all frequency channels are listed in Table 1.

*3.2. Data Format and Channel Power Calculation.* The instantaneous RF power of each frequency point within the frequency channel of interest was measured with a 1 millisecond time step. The data structure of the measurement is shown in Table 2. According to the channel power calculation algorithm of the spectrum analyzer, the measured RF power in dBm of each frequency point is converted to the unit of milliwatt. The instantaneous power of the time sampling point $i$ and the frequency sampling point $j$ is referred to as $pij(mW)$ in Table 2. To obtain the channel power, measured RF power of all frequency points in the channel are summed and converted back to dBm. The instantaneous channel power of the time sampling point $i$ is referred to as $P_i$ in Table 2 in the rightmost column. With the input power of the frequency channel and the average antenna gain, the power density can be calculated using equation (3).

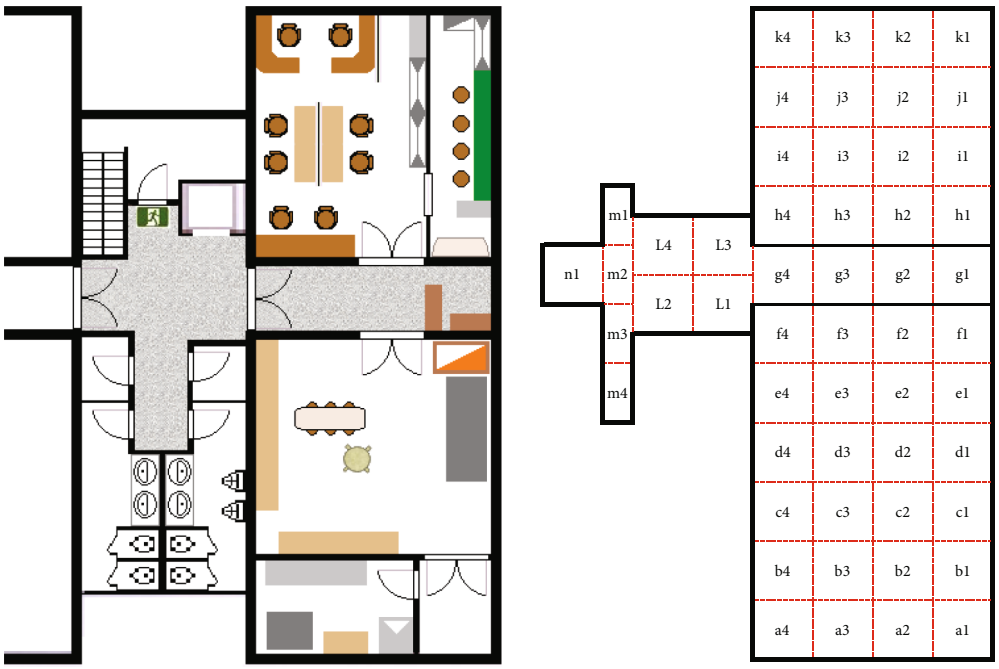


Figure 3: Measurement area of the ambient RF power and coordinates of all measurement positions.

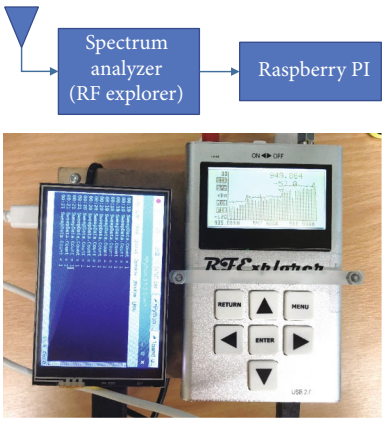


Figure 4: Block diagram and photograph of the low-cost ambient RF power measurement system.

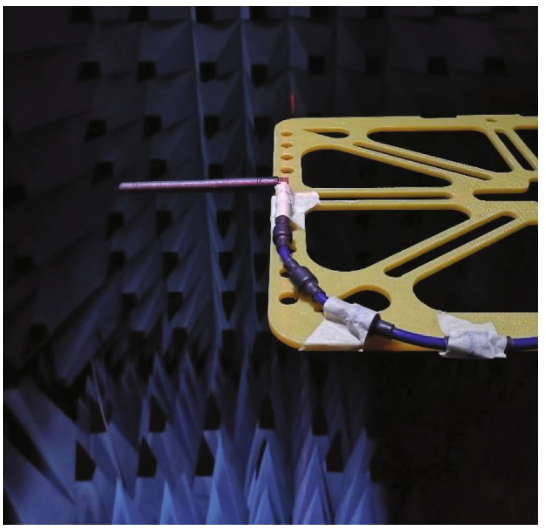

Figure 5: Characterization of the monopole antenna used for the survey.

*3.3. Normalization of the Channel Power.* The instantaneous channel power from Table 2 is a function of the frequency dependent gain of the monopole antenna used for the survey. For a fair comparison of the available RF power of all frequency channels, the measured RF power must be normalized so that the antenna gain is excluded from the measured values. The estimated RF input power $P_{\mathrm{INest}}$ is given with

$$P_{\mathrm{INest}} = G_0 \frac{\lambda^2}{4\pi} s_t. \tag{4}$$

where $G_0$ is the isotropic gain which is 1 and $s_t$ is the power density that can be calculated using equation (3). Substituting (3) into (4) leads to

$$P_{\mathrm{INest}} = \frac{G_0}{G_{\mathrm{mono}}} P_{\mathrm{INraw}}. \tag{5}$$

According to the algorithm provided by the spectrum analyzer, the estimated channel power $P_{\mathrm{CHest}}$ with $m$ frequency sampling points is given by

$$P_{\mathrm{CHest}}(mW) = P_{\mathrm{INest\_1}}(mW) + P_{\mathrm{INest\_2}}(mW) + \cdots + P_{\mathrm{INest\_m}}(mW), \tag{6}$$

Table 1: Average gain of the monopole antenna used for the survey in all frequency channels of interest.

| Frequency channel | 869-894 MHz | 940-960 MHz | 1,805-1,880 MHz | 2,110-2,170 MHz |
|---|---|---|---|---|
| Average gain of the monopole in dBi | -2.03 | -1.42 | -0.53 | -2.99 |

Table 2: Data format of the RF power measurement.

| Time/frequency sampling | $f_1$ | $f_2$ | .. . | $f_m$ | Channel power (dBm) |
|---|---|---|---|---|---|
| $t_1$ | $p_{11}$ (mW) | $p_{12}$(mW) | .. . | $p_{1m}$ (mW) | $P_1 = 10 \log \sum_{i=1}^{m} p_{1i}$ |
| $t_2$ | . | . | .. . | $p_{2m}$ (mW) | $P_2 = 10 \log \sum_{i=1}^{m} p_{2i}$ |
| . | . | . | | . | . |
| . | . | . | .. . | . | . |
| . | . | . | | . | . |
| $t_n$ | $p_{n1}$ (mW) | $p_{n2}$ (mW) | .. . | $p_{nm}$ (mW) | $P_n = 10 \log \sum_{i=1}^{m} p_{ni}$ |

where $P_{\text{INest\_}i}$ is the estimated power of the frequency point $i$. Substituting (5) into (6) leads to

$$P_{\text{CHest}}(mW) = \frac{G_0}{G_{\text{mono}}} \left( \sum_{i=1}^{m} P_{\text{INraw\_i}}(mW) \right). \quad (7)$$

Considering the power in dBm, equation (7) can be expressed as

$$P_{\text{CHest}}(dBm) = 10 \log \left( \frac{G_0}{G_{\text{mono}}} \right) + 10 \log \left( \sum_{i=1}^{m} P_{\text{INraw\_i}}(mW) \right). \quad (8)$$

The second term of (8) is the channel power measured by the spectrum analyzer. Therefore, (8) can be written as

$$P_{\text{CHest}}(\text{dBm}) = G_0(\text{dBi}) - G_{\text{mono}}(\text{dBi}) + P_{\text{INraw}}(\text{dBm}), \quad (9)$$

where the isotropic gain $G_0$ is 0 dBi. By subtracting the average gain of the monopole antenna used for the survey from the measured RF input power, available RF power of each frequency channel can be evaluated independent of the gain of the antenna used for the survey.

## 4. Survey Results and Rectifier Optimization

It must be noted here that the antenna used for the measurement campaign is linearly polarized. The antenna was oriented to receive signals with vertical polarization. Since polarization of the ambient RF signals is random, the signal power with other polarization was omitted. Thus, the measurement result provides available ambient RF power only for RFEH devices with vertically polarized antennas. To investigate the ambient RF power available from different antenna orientation, the test antenna was also aligned horizontally to receive signals with a horizontal polarization. It was observed that the channel power measured with vertical and horizontal polarization showed a maximum difference of 3 dBm. Even if the test measurement in this work does not cover the signal power of arbitrary polarization, the proposed method to estimate the channel power based on the survey result can be used for rectifier optimization if antennas used for the survey and for RFEH device are of the same type. To measure ambient RF power density independent of signal polarization, a circularly or a dual polarized antenna can be used. To harvest the ambient RF energy from any polarization, a circularly or a dual polarized antenna must also be utilized for RFEH device.

*4.1. Heat Map and Power Estimation.* The channel power in dBm from equation (7) of all measurement positions in the test area can be visualized as heat maps. Figure 6 shows heat maps of all frequency channels from Table 1. The available RF power of each position in the heat map is a time average value over the sampling period of two minutes. The measured RF power has been normalized by the antenna gain used for the survey in each frequency channel from Table 1 for a fair comparison. It can be observed that the frequency channel from 940-960 MHz provides the most promising ambient RF power for energy harvesting compared to other channels.

The position with the maximum time-averaged power is marked by a circle as shown in Figure 6 which is the position j4 from Figure 3. The maximum channel power is -7.6 dBm while the mean value is -11.1 dBm. For RFEH systems, the power conversion efficiency of the rectifier can be optimized only for a certain value of RF input power. However, at a certain place and even for a certain frequency channel, the RF power fluctuates over time. The distribution of the channel power over the measurement time of the position j4 from Figure 3 is shown in Figure 7.

*4.2. Rectifier Optimization Based on Survey Results.* The rectifier must be designed according to the RF power distribution of each location to harvest the highest amount of RF

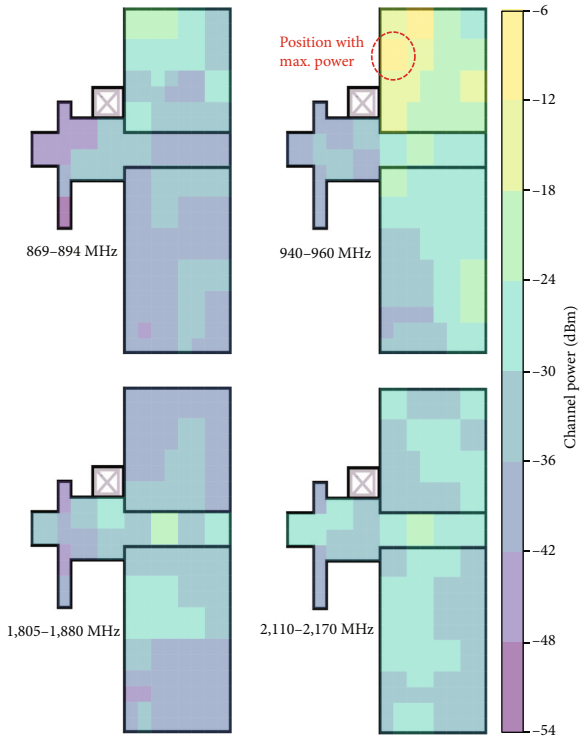


Figure 6: Heat maps of all frequency channels showing average RF power at each position in the test area.

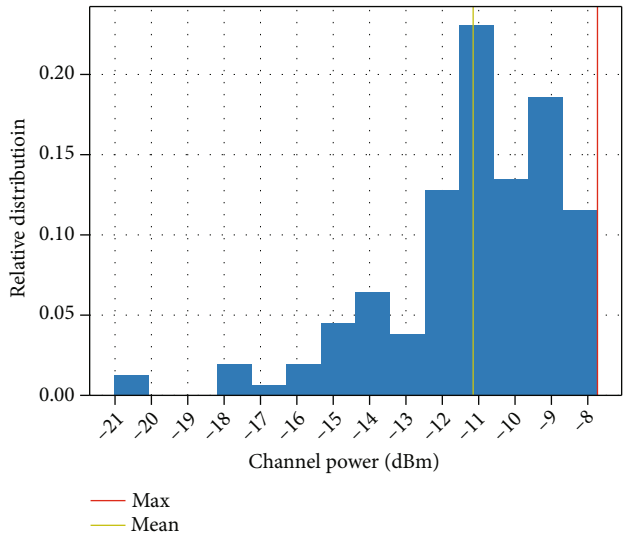


Figure 7: Channel power distribution over the measurement time of the position with the maximum time-averaged RF power.

energy. To verify this concept, a rectifier circuit with the schematic shown in Figure 8 was simulated.

As the input power is increased above the threshold, the diode (Schottky diode SM7621 from Skyworks) is turned on and the diode current starts to flow. At the output, the load RL and storage capacitor (C storage) form a low pass filter so that the RF signal is rectified to DC at the output. This rectifier architecture is referred to as single series-diode which can provide higher PCE at low input power level compared

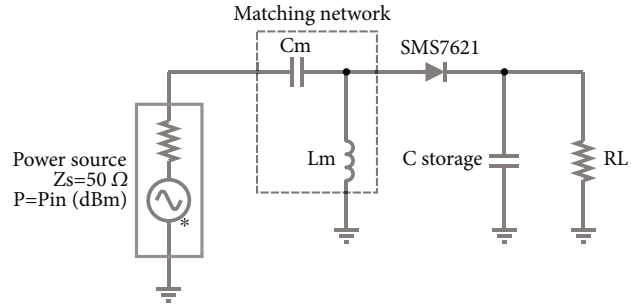


Figure 8: Schematic of a single series-diode rectifier circuit for the PCE optimization study.

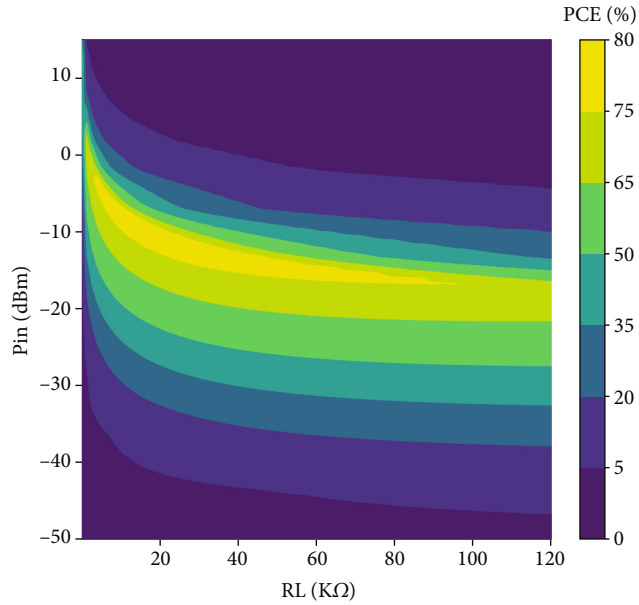


Figure 9: PCE contour for various RF input power and load impedance.

to multiple-diode configuration. The choice of this rectifier architecture is based on the RFEH applications where the expected input power is lower compared to wireless power transfer applications. Alternatively, single shunt-diode architecture can also be considered with a comparable performance and efficiency [33].

In the first step of the optimization, the load RL was varied from zero to 120 kΩ leading to variation of the rectifier's input impedance. A simplified input matching network using a shunt inductor Lm and a series capacitor Cm was designed to match the input impedance of the rectifier to 50 Ohm. Next, the input power of the source was swept from -50 dBm to 15 dBm for each value of RL. For all combinations of RL and input power under a perfect input impedance matching condition, PCE was calculated, and the result is depicted as a PCE contour in Figure 9. Considering this device specific PCE contour, the optimal load RL can be determined to obtain the highest PCE at the nominal input power.

The rectifier's PCE was optimized for the maximum channel power of -7.6 dBm and for the mean RF power of

Table 3: Rectifier circuit parameters and estimated harvested energy after RF to DC conversion.

| Design | PCE optimization case | Nominal pin (dBm) | RL (kΩ) | Cm (pF) | Lm (nH) | Energy (mJ) |
|---|---|---|---|---|---|---|
| Rectifier 1 | Max | -7.6 | 11.2 | 0.26 | 83.3 | 9.9 |
| Rectifier 2 | Mean | -11.1 | 26.15 | 0.18 | 112 | 8.69 |
| Rectifier 3 | Backoff 1 | -17.1 | 91.21 | 0.1 | 163 | 2.84 |
| Rectifier 4 | Backoff 2 | -14.7 | 69.94 | 0.12 | 150 | 3.82 |
| Rectifier 5 | Backoff 3 | -9.0 | 15.8 | 0.23 | 93.8 | 9.93 |

-11.1 dBm (see Figure 7). In addition, three other values of the backoff power including -17.1 dBm (backoff 1), -14.7 dBm (backoff 2), and -9.0 dBm (backoff 3) were also simulated to optimize the PCE (see Rectifier 1–Rectifier 5 in Table 3). The circuit design parameters are shown in Table 3. Simulated S11 values of the impedance matched rectifiers from Table 3 are shown in Figure 10. In case of Rectifier 3 and 4, the sudden change of S11 to total reflection at the frequencies of 953.5 MHz and 957 MHz, respectively, is due to the low pass filter effect of the high load impedance in case of low RF input power and the junction capacitor of the diode. If the junction capacitor is excluded from the diode model, S11 graphs of Rectifiers 3 and 4 show smooth frequency responses like the other designs.

To investigate the robustness of the rectifiers' input matching to fluctuation of the input power, input reflection coefficient of Rectifier 1 and Rectifier 2 were simulated with different values of power backoff from the nominal input power. The simulation results are shown in Figures 11 and 12 for Rectifier 1 and Rectifier 2, respectively.

From Figures 11 and 12, it is observed that the input matching is degraded as the input power fluctuates. For Rectifier 1, magnitude of S11 is lower than -10 dB for 5 dB, 10 dB, and 15 dB power backoff. With 20 dB backoff, magnitude of S11 is approximately -6 dB at the center frequency of the channel. In case of Rectifier 2 with a lower nominal input power, a good matching is provided with 10 dB backoff. With 5 dB and 15 dB backoff, magnitude of S11 is higher than -10 dB at the center frequency of the channel. Degradation of the input matching due to power fluctuation leads to lower RF power being rectified by the diode and consequently to a lower PCE. In addition, as the input power decreases, the load resistance optimized for the nominal input power is no longer optimal for lower input power. The PCE graphs of all 5 rectifiers with different nominal values of RF input power are shown in Figure 13.

According to

$$P_{DC} = \text{PEC} \times P_{IN}, \tag{10}$$

where $P_{IN}$ is the input power which fluctuates over time according to the distribution in Figure 5, the DC output power $P_{DC}$ can be calculated for each rectifier design based on expected value of $P_{IN}$. By substituting the channel power $P_{CHest}$ from equation (7) as the input power of equation (8) and with the simulated PCE of each rectifier design from Figure 13, the DC output power over time can be plotted in Figure 14. To compare the performance of each rectifier based on estimated input power with an isotropic antenna,

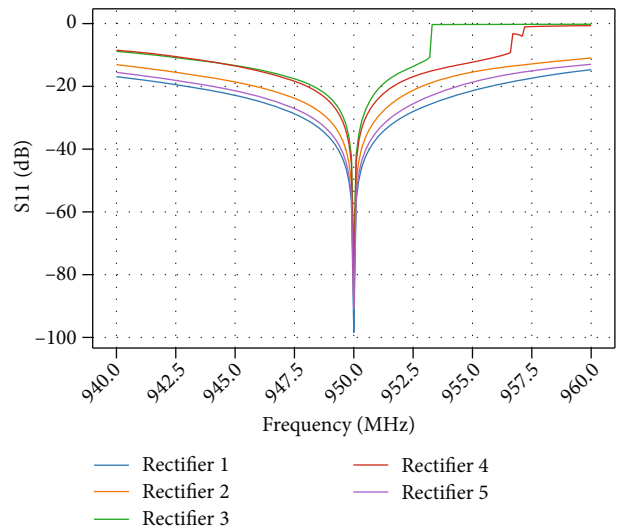


Figure 10: Simulated S11 (magnitude) of the rectifiers from Table 3 with different values of nominal RF input power.

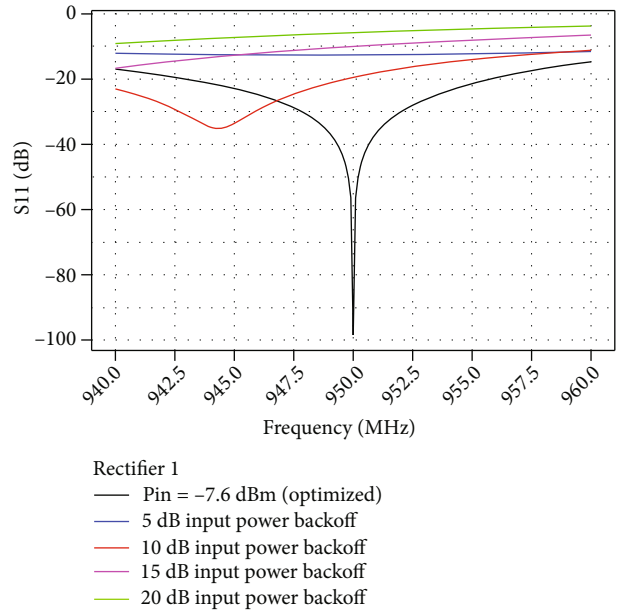


Figure 11: Simulated S11 (magnitude) of Rectifier 1 with different power backoffs from the nominal RF input power.

the total energy within the testing period was calculated by integrating the graph in Figure 14 overtime. The harvested RF energy of each rectifier design are shown in the right most column of Table 3.

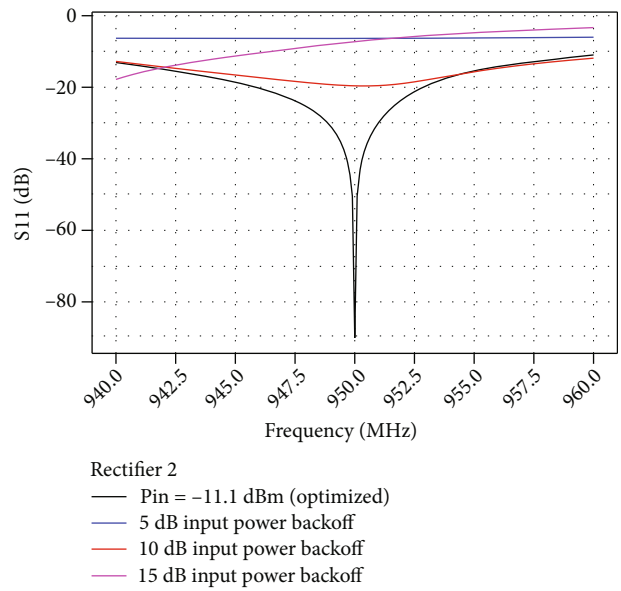


Figure 12: Simulated S11 (magnitude) of Rectifier 2 with different power backoffs from the nominal RF input power.

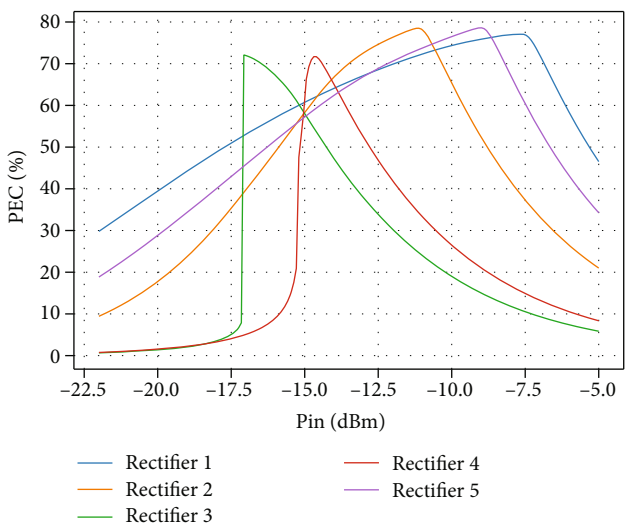


Figure 13: PCE simulation results optimized for various nominal RF input power including -7.6 dBm (max), -11.1 dBm (mean), -17.1 dBm (backoff 1), -14.7 dBm (backoff 2), and -9.0 dBm (backoff 3).

## 5. Discussion

This survey focused mainly on a short test period which represents a typical profile of channel power that can be harvested using a RFEH system. If a longer survey period is necessary, the developed measurement system can also be left at the test positions for longer time. From the survey, it is observed that the channel power has a mean value of -11.1 dBm which was detected the most during the survey time. The maximum channel power from the survey was -7.6 dBm. However, this value was detected less often during

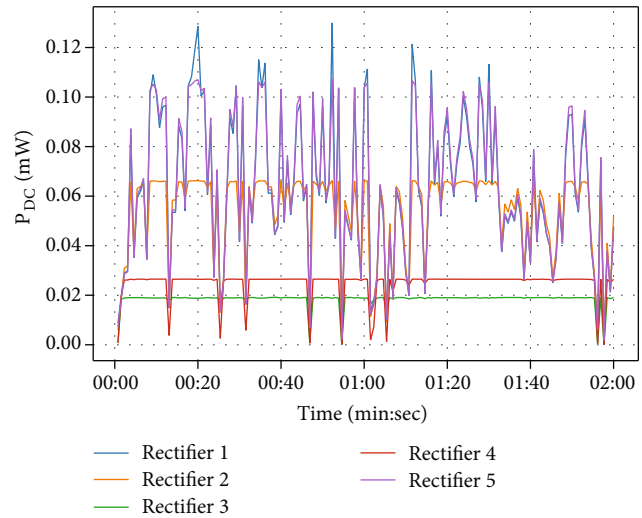


Figure 14: Estimated DC output power over time from field test measurement for each optimal input power of the rectifier.

the survey compared to the mean value. According to the survey result, if the rectifier is optimized based on mean value of the channel power (Rectifier 2 in Table 3), PCE drops rapidly as the input power exceeds the optimal input power. This is not the case if the maximum value from the survey is used for the optimization (Rectifier 1 in Table 3) since there is very low possibility that the optimal input power is exceeded. Considering PCE degradation due to the power back off from the optimal point, Rectifier 2 shows a stronger decrease of PCE compared to Rectifier 1. At the optimal input power of Rectifier 2, Rectifier 1 provides a slightly lower PCE. However, as input power decreases to -15 dBm, Rectifier 1 provides a larger PCE than that of Rectifier 2. In case of Rectifiers 4 and 5, the optimal input power is lower than the mean value and the harvested energy is very low (see Figure 8 and the right most column of Table 3). In contrast, the input power of Rectifier 3 is optimized at -9 dBm which is between -7.6 dBm and -11.1 dBm in case of Rectifier 1 and 2, respectively. This design provides the best value of harvested RF energy among all designs.

For the survey result in this work, it is observed that the optimal input power of the rectifier should be between the mean and the maximum value. Since another survey at a different test area and at a different time will provide a different RF input power distribution other than Figure 5, it is important to acquire information regarding available RF input power prior to the rectifier design process. Our study also shows that a rectifier with an optimal input power below the mean value from the survey is not practical. This is because harvestable RF power below the mean is extremely low. Besides, if RF power higher than the optimal value is fed to the rectifier, PCE will be very small due to the breakdown effect. Simulated PCE as a function of RF input power from Figure 13 can be multiplied with the power distribution from Figure 7 to estimate the DC power converted from RF input power by the rectifier. An optimum nominal RF input power can be chosen to maximize the harvested ambient RF

Table 4: Comparison of ambient RF power survey and other works in the literature.

| Related work | Survey dedicated for RFEH | Information for rectifier design | Typical RF power | Key feature of rectifier |
|---|---|---|---|---|
| Piñuela et al. [11] | Yes | Frequency band | -29 to -12 dBm | Multiband |
| Muncuk et al. [12] | Yes | Frequency band | -24 to -5 dBm | Multiband |
| Adegoke et al. [13] | Yes | No | -70 to -99.5 dBm/cm$^2$ | — |
| Watanabe and Hamaba [14] | No | No | 78 to 99 dBuV/m | — |
| Visser et al. [16] | Yes | No | 0.3 to 3 mW/m$^2$ | — |
| This work | Yes | Power distribution | -21 to -7.6 dBm | Optimization based on power distribution |

energy. This first step of choosing an optimal nominal RF input power must be carried out before applying other sophisticated PCE enhancement techniques e.g., harmonic termination for the rectifier design. Comparison of ambient RF power surveys reported in the literature is shown in Table 4.

## 6. Conclusions and Future Work

In this work, harvested ambient RF energy converted to DC by a single stage rectifier has been estimated from survey results of ambient RF power. The measured ambient RF power has been normalized in such a way that it is independent of the antenna used for the measurement. The channel power of the signal with a center frequency of 950 MHz and 20 MHz bandwidth was measured using an in-house developed measurement system consisting of a low-cost spectrum analyzer and a raspberry PI model B+. A distribution of ambient RF power over the measurement time was created for the test area. At the best position, the maximum channel power was -7.6 dBm whereas the mean value with highest channel power statistic was -11.1 dBm. A single stage rectifier circuit was simulated to find the nominal RF input power as a design parameter of the rectifier circuit according to the survey result. From the survey and simulation, the rectifier should be designed to provide a maximum RF to DC power conversion efficiency at an input power of -9 dBm which is between the mean and the maximum values to harvest the highest amount of ambient RF energy. A measurement survey of ambient RF power distribution should be carried out prior to the rectifier design process to determine the nominal RF input power for PCE optimization. From the estimated DC energy converted from the ambient RF energy, it can also be assessed what kind of applications can be realized based on harvestable RF energy in the area of interest. In a future work, a single stage rectifier which can be reconfigured for various RF input power level will be designed and tested at different locations with different ambient RF power distribution. A higher level of RF input power is expected in case of an outdoor scenario which is not covered in this work. To be able to apply the rectifier for both indoor and outdoor scenarios, high PCE must be maintained for a wide dynamic range e.g., by applying the concept of adaptive signal path with dedicated matching for indoor and outdoor scenarios.

## Data Availability

The data that support the finding of this study are available from the corresponding author, Chalermwisutkul, S. upon reasonable request.

## Conflicts of Interest

The authors declare no conflict of interest.

## Acknowledgments

This research was funded by the Research and Researchers for Industries (RRi) Ph.D. Scholarship awarded by the National Research Council of Thailand (NRCT) with the contract number PHD60I0073. Also, this research was funded the Thailand Science Research and Innovation Fund, and the King Mongkut's University of Technology North Bangkok with contract no. KMUTNB-FF-65-42.

## References

[1] H. A. Sodano, G. E. Simmers, R. Dereux, and D. J. Inman, "Recharging batteries using energy harvested from thermal gradients," *Journal of Intelligent Material Systems and Structures*, vol. 18, no. 1, pp. 3–10, 2007.

[2] S. Roundy, P. K. Wright, and J. Rabaey, "A study of low level vibrations as a power source for wireless sensor nodes," *Computer Communications*, vol. 26, no. 11, pp. 1131–1144, 2003.

[3] T. G. Ma, Z. H. Liu, Y. W. Chang, and H. N. Chu, "Metamaterial self-oscillating active antennas for extending readable range of RFID," in *2018 International Symposium on Antennas and Propagation (ISAP 2018)*, pp. 193-194, Busan, Korea, October 2018.

[4] Z. Meng and Z. Li, "RFID tag as a sensor - a review on the innovative designs and applications," *Measurement science review*, vol. 16, no. 6, pp. 305–315, 2016.

[5] M. Bunruangses, A. E. Arumona, P. Youplao et al., "Realizing THz RFID using silicon chip space-time control circuit," *SILICON*, vol. 13, no. 10, pp. 3725–3732, 2021.

[6] F. Mazunga and A. Nechibvute, "Ultra-low power techniques in energy harvesting wireless sensor networks: recent advances and issues," *Scientific African*, vol. 11, article e00720, 2021.

[7] J.-T. Kim, B.-R. Heo, and I. Kwon, "An energy-efficient UWB transmitter with wireless injection locking for RF energy-harvesting sensors," *Sensors*, vol. 21, no. 4, p. 1426, 2021.

[8] T. R. Kumar and M. Madhavan, "Design and Implementation of Wearable Microstrip Fabric Antenna for RF Energy

Harvesting," *International Journal of Engineering Research and Technology*, vol. 10, no. 1, 2017.

[9] P. Spies, M. Pollak, and L. Mateu, *Handbook of Energy Harvesting Power Supplies and Applications*, CRC Press, 2015.

[10] J. M. Gilbert and F. Balouchi, "Comparison of energy harvesting systems for wireless sensor networks," *International Journal of Automation and Computing*, vol. 5, no. 4, pp. 334–347, 2008.

[11] M. Piñuela, P. D. Mitcheson, and S. Lucyszyn, "Ambient RF energy harvesting in urban and semi-urban environments," *IEEE Transactions on microwave theory and techniques*, vol. 61, no. 7, pp. 2715–2726, 2013.

[12] U. Muncuk, K. Alemdar, J. D. Sarode, and K. R. Chowdhury, "Multiband ambient RF energy harvesting circuit design for enabling batteryless sensors and IoT," *IEEE Internet of Things Journal*, vol. 5, no. 4, pp. 2700–2714, 2018.

[13] E. I. Adegoke, R. M. Edwards, W. Whittow, and A. Bindel, "RF power density measurements for RF energy harvesting in automobile factories," in *2015 Loughborough Antennas & Propagation Conference (LAPC)*, pp. 1–5, Loughborough, UK, November 2015.

[14] S. Watanabe and L. Hamada, "3-4 measurements of the electromagnetic field from a Mobile Phone Base station," *Journal of the National Institute of Information and Communications Technology*, vol. 63, no. 1, pp. 213–231, 2017.

[15] J. Higashiyama and Y. Tarusawa, "Evaluating RF Field Intensity in Mobile Base Station Environment," *NTT DOCOMO Technical Journal*, vol. 16, no. 3, pp. 27–34, 2015.

[16] H. J. Visser, A. C. F. Reniers, and J. A. C. Theeuwes, "Ambient RF energy scavenging : GSM and WLAN power density measurements," in *2008 38th European Microwave Conference*, pp. 721–724, Amsterdam, Netherlands, October 2008.

[17] M. Alibakhshikenari, B. S. Virdee, C. H. See, R. A. Abd-Alhameed, F. Falcone, and E. Limiti, "Energy harvesting circuit with high RF-to-DC conversion efficiency," in *2020 IEEE International Symposium on Antennas and Propagation and North American Radio Science Meeting*, pp. 1299-1300, Montreal, QC, Canada, 2020.

[18] S. Muhammad, A. Smida, M. I. Waly et al., "Design of wideband circular-slot antenna for harvesting RF energy," *International Journal of Antennas and Propagation*, vol. 2022, Article ID 5964753, 9 pages, 2022.

[19] H. Sun, Y. X. Guo, M. He, and Z. Zhong, "A dual-band rectenna using broadband yagi antenna array for ambient rf power harvesting," *IEEE Antennas and Wireless Propagation Letters*, vol. 12, pp. 918–921, 2013.

[20] S. Shen, Y. Zhang, C.-Y. Chiu, and R. Murch, "An ambient RF energy harvesting system where the number of antenna ports is dependent on frequency," *IEEE Transactions on Microwave Theory and Techniques*, vol. 67, no. 9, pp. 3821–3832, 2019.

[21] C. Song, Y. Huang, J. Zhou, S. Yuan, Q. Xu, and P. Carter, "A broadband efficient rectenna array for wireless energy harvesting," in *2015 9th European Conference on Antennas and Propagation (EuCAP)*, pp. 10–14, Lisbon, Portugal, 2015.

[22] T. W. Yoo and K. Chang, "Theoretical and experimental development of 10 and 35 GHz Rectennas," *IEEE Transactions on Microwave Theory and Techniques*, vol. 40, no. 6, pp. 1259–1266, 1992.

[23] K. Arpanutud, M.-D. Wei, K. Phaebua, S. Tontisirin, R. Negra, and S. Chalermwisutkul, "Adaptive piecewise linear model for class C rectifier design," *International Journal of Numerical Modelling: Electronic Networks, Devices and Fields*, vol. 35, article e2943, 2022.

[24] V. Jantarachote, S. Tontisirin, P. Akkaraekthalin, R. Negra, and S. Chalermwisutkul, "CMOS rectifier design for RFID chip with high sensitivity at low input power to be combined with an ultrasmall antenna," *International Journal of Numerical Modelling: Electronic Networks, Devices and Fields*, vol. 32, no. 6, 2019.

[25] C. A. Balanis, *Antenna Theory*, Wiley-Interscience, 3rd edition, 2005.

[26] S. Muhammad, J. J. Tiang, S. K. Wong, A. Iqbal, M. Alibakhshikenari, and E. Limiti, "Compact rectifier circuit design for harvesting gsm/900 ambient energy," *Electronics*, vol. 9, no. 10, p. 1614, 2020.

[27] D. Khan, M. Basim, K. Shehzad et al., "A 2.45 GHZ high efficiency CMOS RF energy harvester with adaptive path control," *Electronics*, vol. 9, no. 7, pp. 1107–1114, 2020.

[28] E. M. Abdelhady, H. M. Abdelkader, and A. A. Al-Awamry, "Self-Adaptive rectenna with high efficiency over a wide dynamic range for RF energy harvesting applications," *The Journal of Communication*, vol. 16, no. 2, pp. 67–75, 2021.

[29] "P2110B 915 MHz RF Powerharvester® Receiver, Datasheet," https://www.powercastco.com/wp-content/uploads/2016/12/P2110B-Datasheet-Rev-3.pdf.

[30] F. Bolos, J. Blanco, A. Collado, and A. Georgiadis, "RF energy harvesting from multi-tone and digitally modulated signals," *IEEE Transactions on Microwave Theory and Techniques*, vol. 64, no. 6, pp. 1918–1927, 2016.

[31] A. Litvinenko, S. Tjukovs, D. Pikulins, and A. Aboltins, "The impact of waveform on the efficiency of wireless power transfer using prefabricated energy harvesting device," in *2018 International Conference on Information and Telecommunication Technologies and Radio Electronics (UkrMiCo)*, Odessa, Ukraine, 2018.

[32] *RF explorer*http://j3.rf-explorer.com/.

[33] S.-P. Gao and H. Zhang, "Topology comparison of single-diode rectifiers: shunt diode vs. series diode," in *2019 12th International Workshop on the Electromagnetic Compatibility of Integrated Circuits (EMC Compo)*, pp. 177–179, Hangzhou, China, 2019.